National Aeronautics and Space Adminstration

Kinetic Monte Carlo Simulation of Oxygen Diffusion in Ytterbium Disilicate

Brian S. Good, Materials and Structures Division, NASA Glenn Research Center, Cleveland, OH

Introduction

Silicon-based ceramic components for next-generation jet turbine engines offer potential weight savings, as well as higher operating temperatures, both of which lead to increased efficiency and lower fuel costs. Silicon carbide (SiC), in particular, offers low density, good strength at high temperatures, and good oxidation resistance in dry air. However, reaction of SiC with high-temperature water vapor, as found in the hot section of jet turbine engines in operation, can cause rapid surface recession, which limits the lifetime of such components. Environmental Barrier Coatings (EBCs) are therefore needed if long component lifetime is to be achieved.

Rare earth silicates such as $Yb_2Si_2O_7$ and Yb_2SiO_5 have been proposed for such applications; in an effort to better understand diffusion in such materials, we have performed kinetic Monte Carlo (kMC) simulations of oxygen diffusion in Ytterbium disilicate, $Yb_2Si_2O_7$. The diffusive process is assumed to take place via the thermally activated hopping of oxygen atoms among oxygen vacancy sites or among interstitial sites. Migration barrier energies are computed using density functional theory (DFT).

β-YTTERBIUM DISILICATE STRUCTURE

β-Ytterbium disilicate exists in a distorted monoclinic phase that is stable from near room temperature to at least 1600C. The space group is C2/m (12), with lattice parameters a = 6.802Å, b = 8.875Å, c = 4.703Å, α = 90.0°, β = 102.12°, γ = 90.0°.

The unit cell, which contains two eleven-atom $Yb_2Si_2O_7$ chemical units, is shown in Figure 1. All oxygen atoms are contained within a double-tetrahedron structure, with the two tetrahedra sharing a common oxygen atom. There are three distinct oxygen sites, with different symmetries, and therefore different coordination.

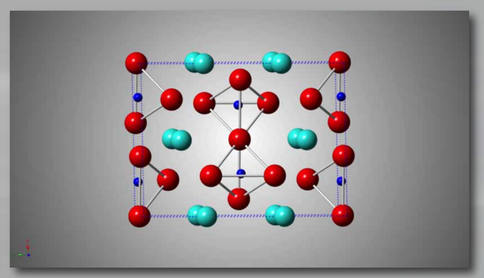

Figure 1— $Yb_2Si_2O_7$ structure, (001) plane. Yb (light blue), Si (dark blue), Oxygen (red). In each tetrahedron, type O1 atoms are shared with another tetrahedron. Of the remaining three atoms, one is type O2 and two are type O3.

KINETIC MONTE CARLO METHOD

- The kMC method is designed to investigate the dynamical evolution of a system.
- It is particularly well suited for the study of "infrequent event" systems, in which the events of interest are widely separated spatially or temporally.
- It treats the events of interest in detail while incorporating only the average behavior of the system between events.
- It is often substantially more efficient than molecular dynamics simulations for such systems.

KMC procedure for diffusive hopping

- Events of interest are thermally activated diffusive hops among vacancy or interstitial sites. Migration barrier energies were computed using density functional theory (DFT). All hops are assumed to be uncorrelated.
- A Yb disilicate computational cell is created that includes vacancy and interstitial concentrations appropriate for the simulation temperature.
- All potential hops within the cell are identified and the event hopping rates are computed as $\nu_{AB}=\nu^0 \exp\left(-\frac{E_{AB}}{k_B T}\right)$ in which ν_{AB} and E_{AB} are the hopping rate and migration barrier energy for a hop between lattice or interstitial sites A and B respectively, and ν^0 is the frequency factor, typically assumed to be between 10^{12} and 10^{13}.

KMC procedure for diffusive hopping (continued)

- The probability for each possible hop can be computed from the hopping rate, with $P_{AB}=\frac{\nu_{AB}}{\Gamma}$, where Γ is the sum of hopping rates for all possible hops in the computational cell. Event displacement vectors and probabilities for all hops accessible to the system are included in an event catalog.
- An event is chosen from the catalog stochastically, based on the event probabilities, and executed. The execution of such an event makes a number of new events accessible to the system, while a number of previously-accessible events become inaccessible.
- Event probabilities for the newly-accessible events are computed. The newly-accessible events and probabilities are added to the event catalog, and the newly-inaccessible events and probabilities are deleted.
- The simulation clock is advanced stochastically by an amount by $\Delta t = -\frac{\ln(R)}{\Gamma}$ where R is a random number, $0 < R <= 1$.
- The process proceeds until an appropriate number of events have been executed.
- When the simulation has finished, the total elapsed time, t, and the mean square displacement, $<R^2>$, averaged over all vacancies, is computed.
- The diffusivity D is obtained from the Einstein relation $<R^2> = 6Dt$.
- In the case of vacancy-mediated diffusion, it is convenient to track vacancies rather than oxygen atoms. In this case the oxygen diffusivity DO is obtained by balancing the number of vacancy and atomic hops:
  $D_O = \frac{C_v}{1-C_v} D_v$ where C_v is the concentration of vacancies.

Results and Discussion

The lattice constant a was optimized using DFT, assuming the ratios *b/a* and *c/a* and angle β were as reported by Smolin. AI calculations were performed using the VASP density functional code, with projector augmented wave pseudopotentials, and using the generalized gradient approximation (GGA). The value obtained was 7.043Å, larger than value reported by Smolin by 3.5%, consistent with DFT-GGA's tendency to underbind.

Vacancy-mediated diffusion

Vacancy site preferences were determined by computing the energies of relaxed unit cells having
vacancies at O1, O2 and O3 sites. The O1 site is lowest in energy, and the O2 and O3 site energies were larger by 0.68eV and 0.61eV, respectively.

Vacancy formation energies were found to be 3.59eV, 4.0eV and 4.20eV for the O1, O2 and O3 vacancy sites, respectively. The intrinsic concentrations of vacancies at the three oxygen site types were computed as $C_c = \exp\left(-\frac{E_{vf}}{k_B T}\right)$. The values range from $O(10^{-19})$ at 1000K to $O(10^{-19})$ at 2000K. In all cases, the intrinsic vacancy concentration is so small that oxygen permeation in the pristine material is unlikely to be problematic.

Diffusion Paths and Barrier Energies

Oxygen coordination histograms for the three oxygen site types are shown in Figure 2a-c. O1 sites have the simplest coordination, with nearest neighbors lying within the two tetrahedra that form the Si_2O_7 complex.

O2 and O3 sites show more complex coordination. Within the same tetrahedron, the O1-O2 and O1-O3 distances are slightly smaller than O2-O3 and O3-O3 distances, indicating a distorted structure. A second neighbor shell involves atoms in other complexes, but the interatomic distances are not much larger than the intra-tetrahedral ones. The O2 site's third neighbor shell is much further away, while the O3 sites show neighbors lying within a broad range of distances.

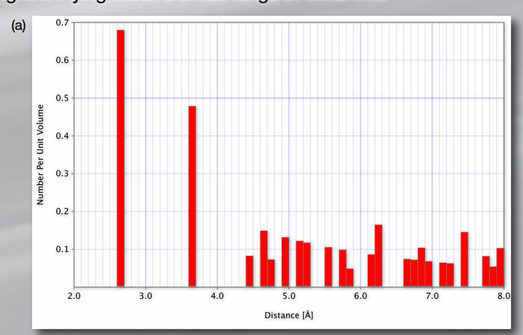

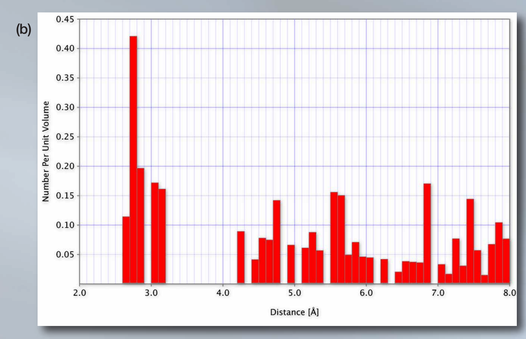

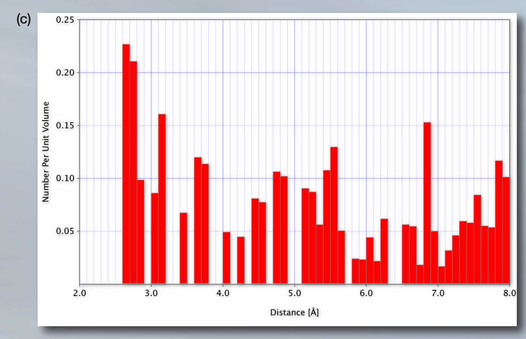

Figure 2—Oxygen coordination histograms for oxygen sites (a) O1, (b) O2, (c) O3.

Because the coordination of the three types of oxygen atoms is complex, we have investigated a variety of potential diffusion paths. We consider three types of paths:

(1) Paths connecting atoms within a single tetrahedron.
(2) Paths connecting atoms in different tetrahedra of a double tetrahedron complex.
(3) Paths connecting atoms in different double tetrahedron complexes.

Paths were defined by the initial site occupied by a hopping atom, the saddle point along the path, and the vacancy site occupied by the hopping atom at the end of the hop.

Paths shorter than 5.3Å (10 bohrs) connecting all possible pairs of oxygen site types were considered, including paths in periodic image cells.

Saddle points were determined using a simple gradient-driven search. A small number of saddle points was investigated using the Climbing Image Nudged Elastic Band (CI-NEB), but the method is computationally too expensive to use with such a large number of paths.

Most of the barrier energies computed were in the range of 1-3eV, with a small number less than 1eV, and a larger number greater than 3eV. A number of low-energy multi-hop paths, for which the largest barrier energy was in the range of 1-2eV, were identified. However, the kMC simulations incorporated all paths, regardless of the barrier energy values.

The lowest-energy paths for each possible interatomic path are shown in Table 1. Within a tetrahedron, the lowest-energy paths are the O3-O3 and O2-O3 sites. The barriers for paths including an O1 site are substantially larger, indicating that diffusive hops involving O3 sites are the most probable. Hopping paths between sites on different tetrahedra in the same complex are in general not energetically favorable. Intercomplex hops involving O1-O3, O2-O2 and O2-O3 paths are higher in energy than the most intracomplex hops, indicating that intercomplex hops will likely be the rate-limiting process.

Path type	Location	Forward barrier, eV	Reverse barrier, eV
O1–O2	same tetrahedron	1.42	2.01
O1–O3	same tetrahedron	1.01	1.50
O2–O3	same tetrahedron	0.64	0.74
O3–O3	same tetrahedron	0.46	same
O2–O2	different tetrahedra, same complex	occluded	
O2–O3	different tetrahedra, same complex	>5	>5
O3–O3	different tetrahedra, same complex	occluded	
O1–O1	different complexes	no low-energy path	
O1–O2	different complexes	>5	4.89
O1–O3	different complexes	1.66	2.23
O2–O2	different complexes	2.13	same
O2–O3	different complexes	1.82	2.33
O3–O3	different complexes	3.53	same

Table 1—Low-energy hopping paths

KMC Simulations

A kinetic Monte Carlo code developed in our laboratory was used, along with the energy barriers as described above. Simulations were performed at temperatures of 1000K,1250K,1500K,1750K and 2000K, with 1750K being close to the target operating temperature of components to be protected by these coatings. Each run consisted of 5 x 10^9 events, and each diffusivity is an average over ten runs.

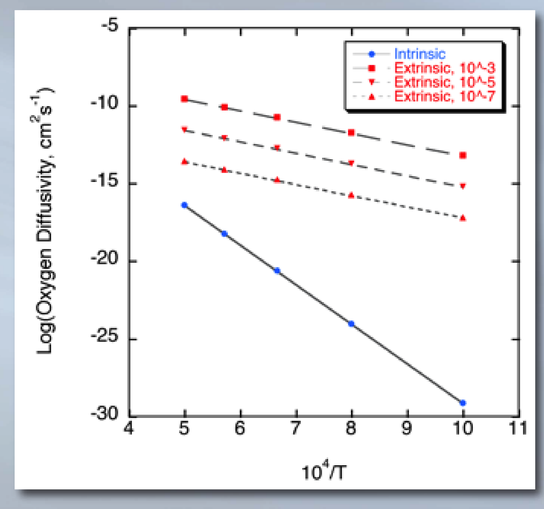

Figure 3—Vacancy-mediated oxygen diffusivities

The results for both the intrinsic vacancy concentration, and a number of fixed assumed extrinsic concentrations of 10^{-7}, 10^{-5} and 10^{-3}, are shown in Figure 3. It is clear that when only intrinsic vacancies are present, the oxygen diffusivity is very small.

Interstitial Diffusion

Defect formation energies for oxygen atoms located at various interstitial sites were computed. The formation energy in this case is defined as the difference between the energy of a cell containing an interstitial atom, and the sum of the energies of a perfect cell and an oxygen atom in its reference state. Three stable interstitial points were identified via structural minimization, and the interstitial formation energy was calculated for each, with values between 1.4 eV and 2.3 eV. The magnitude of these energies indicates that the concentration of interstitial oxygen, while larger than the concentration of vacancies, will still be relatively low.

Interstitial migration barriers were computed for several possible diffusion paths; the migration barriers are about 1eV, indicating that the diffusivity is considerably larger than is the case for vacancy-mediated diffusion, and this has been confirmed in preliminary kMC simulations.

When both the diffusivity and interstitial concentration are considered, it appears that the interstitial diffusive flux through the material will be larger than the vacancy-mediated flux, but will be small enough that it will likely not be of major concern for the proposed application.

Conclusions

Vacancy-mediated oxygen diffusivities from kinetic Monte Carlo simulations are small, as long as only intrinsic oxygen vacancies are considered. The addition of extrinsic vacancies to the simulations can produce diffusivities orders of magnitude larger, though it is not known whether such vacancies exist in the required numbers in the real material.

Predicted interstitial diffusivities are considerably larger than vacancy mediated diffusivities. The interstitial defect formation energies are positive, suggesting that the concentration of interstitial defects in $Yb_2Si_2O_7$, while larger than the vacancy concentration, will be small enough that significant oxygen permeability via this mechanism is unlikely to occur.

Yet to be considered are more complex diffusion mechanisms, for example, diffusion along paths connecting vacancy and interstitial sites; this mechanism is currently under investigation.

PS–01530–0215